TOXICOLOGICAL SCIENCES **104(1)**, 210–217 (2008)
doi:10.1093/toxsci/kfn070
Advance Access publication April 1, 2008

Effect of PBPK Model Structure on Interpretation of *In Vivo* Human Aqueous Dermal Exposure Trials

Anayi M. Norman,* John C. Kissel,*,[1] Jeffry H. Shirai,* Joseph A. Smith,* Kelly L. Stumbaugh,* and Annette L. Bunge†

University of Washington, Seattle, Washington 98105; and †Colorado School of Mines, Golden, Colorado 80401

Received October 17, 2007; accepted March 14, 2008

Multiple research teams have reported data from *in vivo* human trials in which breath was monitored during and after whole-body or partial immersion in aqueous solutions of volatile organic compounds. Estimation of total dermal absorption from exhaled breath measurements requires modeling, a task to which physiologically based pharmacokinetic (PBPK) models have often been applied. In the context of PBPK models, the exposed skin compartment can be modeled in many different ways. To demonstrate potential effects of alternative skin models on overall PBPK model performance, alternative models of skin have been incorporated in a PBPK model used to predict chloroform in breath during and after immersion in aqueous solution. The models investigated include treatment of skin as both a homogeneous phase and as a membrane in which concentration varies with depth. Model predictions are compared with *in vivo* human experimental results reported in the prior literature. In the example chosen, the common practice of modeling skin as a homogenous phase leads to prediction of more rapid initial uptake and lower cumulative uptake than does modeling skin as a membrane. Numerical estimates of the permeability coefficient are shown to be dependent upon skin model form and temperature of the aqueous solution.

Key Words: **absorption; biomonitoring; breath; model; skin; VOCs.**

Results have been reported from multiple human *in vivo* trials conducted to assess dermal absorption of volatile organic compounds (VOCs) from aqueous solution (Gordon *et al*., 1998; Poet *et al*., 2000a, b; Thrall and Woodstock, 2003; Thrall *et al*., 2002; Xu and Weisel, 2005). Because these experiments utilized VOC concentration in exhaled breath as the indicator of exposure, interpretation requires modeling of the relationship between total VOC absorbed and VOC exhaled. Physiologically based pharmacokinetic (PBPK) models can be and have been applied to this task. Dermal absorption is typically characterized by a compound- and external medium-specific permeability coefficient (K_p). By using K_p as a fitting parameter to match PBPK model predictions to breath data, results from the *in vivo* experiments noted above can be employed to estimate K_p. Values of K_p calculated in this manner can be compared with values obtained using the modified Potts-Guy equation recommended by the U.S. Environmental Protection Agency (EPA) in current guidance (U.S. EPA, 2004). The modified Potts-Guy equation is based on results obtained *in vitro*. If interpreted appropriately, *in vivo* experiments therefore represent a potential check on EPA's estimation method.

Published PBPK models have not routinely included skin as most were developed for investigation of oral or other non-dermal dosing scenarios. However, PBPK models can easily be modified by adding skin compartments. McCarley and Bunge (2001) have reviewed various versions of one- and two-compartment skin models. They distinguish three types of one-compartment model that employ properties of actual skin layers (stratum corneum, viable epidermis, dermis) with respect to transport resistance and storage to represent overall skin function either by assuming particular layers are controlling or negligible or by some sort of averaging of their properties. Two-compartment skin models are typically utilized when neither the stratum corneum nor viable epidermis can be neglected because both contribute to transport resistance or storage. Regardless of the number of compartments in these simple adaptations, internal concentration in each compartment is considered uniform at all locations. The term continuously stirred tank reactor (CSTR) is generally used in chemical engineering to describe a modeled volume in which this condition applies. Although modeling of skin as one or two CSTRs is common, experiments have shown that skin behaves like a membrane (Scheuplein, 1972), that is, concentration of penetrating chemical varies with position. However, because mathematical models treating the skin as a membrane require somewhat more cumbersome mathematics and computing resources, they are less utilized despite their greater plausibility.

For purposes of comparison, three variations of a PBPK model are applied here. In each case, the core of the model is the same, with only treatment of skin altered. The first version, referred to below as the CSTR model, describes skin as a single

[1] To whom correspondence should be addressed at Environmental & Occupational Health Sciences, University of Washington, 4225 Roosevelt Way NE, Suite 100, Seattle, WA 98105-6099. Fax: (206) 543-8123. E-mail: jkissel@u.washington.edu.

© The Author 2008. Published by Oxford University Press on behalf of the Society of Toxicology. All rights reserved.
For permissions, please email: journals.permissions@oxfordjournals.org

Downloaded from https://academic.oup.com/toxsci/article-abstract/104/1/210/1721500
by Centers For Disease Control user
on 23 August 2018

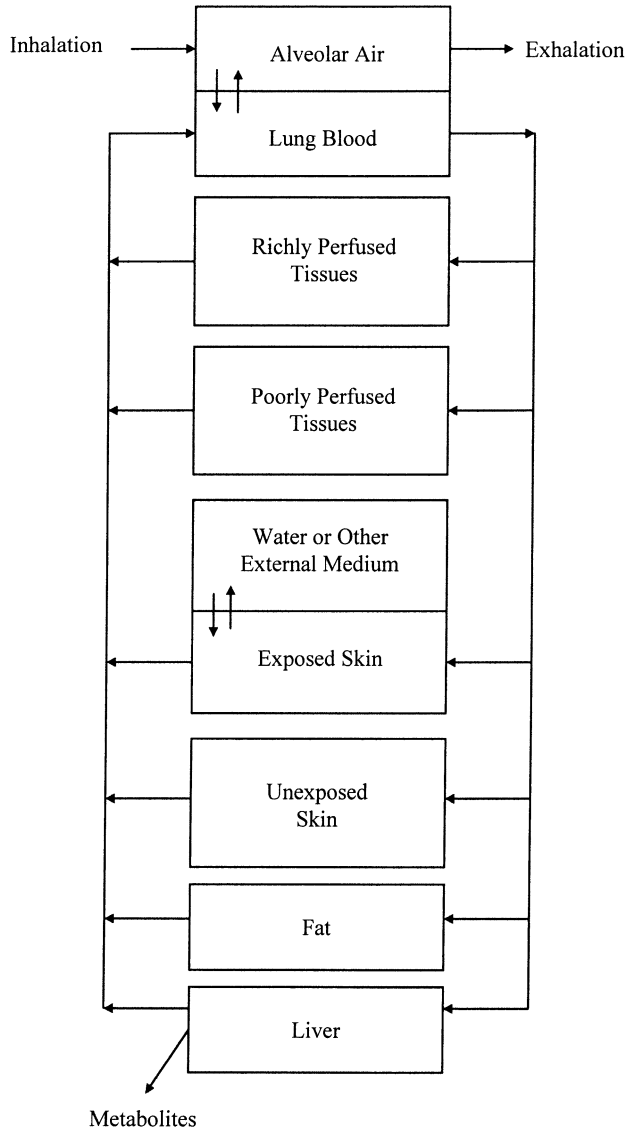

FIG. 1. Schematic of the PBPK framework used here. (In the FD model, the skin compartment is further segmented into 20 layers.)

compartment that is homogeneous with respect to concentration. This approach is common in the prior literature, and merely involves creating a skin compartment analogous to other physiological compartments, which are traditionally modeled as CSTRs. Treatment of skin as a membrane in which a one-dimensional concentration gradient forms is more sophisticated and more consistent with what is known about the physiology of the skin. Because the membrane model used here employs a finite-difference scheme to simulate skin as a membrane, it is referred to as the finite-difference (FD) model. Alternatively, by modifying the CSTR rate constants to match predictions of a membrane model for specific conditions, an approximate membrane model can be created that is computationally simpler than a true membrane model. McCarley and Bunge (1998) have developed several models of this type. The simplified time lag (STL) model is the simplest that contains most of the essential features and is used here to demonstrate the performance of an intermediate skin model form.

TABLE 1
Equations Governing Compartments Other than Exposed Skin

Nonmetabolizing compartments (richly and poorly perfused tissues, fat, unexposed skin):

$$\frac{dC_i}{dt} = \frac{Q_{b,i}}{V_i}\left(C_{artb} - \frac{C_i}{P_{i/b}}\right)$$

C_i = concentration in compartment i (mg/l tissue)
$Q_{b,i}$ = blood flow to compartment i (l/h)
V_i = volume of compartment i (l)
C_{artb} = concentration in arterial blood (mg/l)
$P_{i/b}$ = the tissue i/blood partition coefficient[a]

Liver:

$$\frac{dC_{liver}}{dt} = \frac{Q_{b,liver}}{V_{liver}}\left(C_{artb} - \frac{C_{liver}}{P_{liver/b}}\right) - \frac{v_{max}\frac{C_{liver}}{P_{liver/b}}\rho_{liver}}{K_m + \frac{C_{liver}}{P_{liver/b}}}$$

C_{liver} = concentration in liver tissue (mg/l)
$Q_{b,liver}$ = blood flow to the liver (l/h)
V_{liver} = volume of the liver (l)
C_{artb} = concentration in arterial blood (mg/l)
$P_{liver/b}$ = liver/blood partition coefficient[a]
v_{max} = maximum specific metabolism rate (mg/kg/h)
K_m = Michaelis-Menten coefficient (mg/l blood)
ρ_{liver} = density of the liver (kg/l)

Lung:

$$C_{artb} = \frac{Q_b}{Q_b + \frac{Q_{alv}}{P_{b/a}}}C_{venb}$$

Q_b = cardiac output (l/h)
Q_{alv} = alveolar respiration rate (l/h)
C_{venb} = concentration in venous blood (mg/l)
$P_{b/a}$ = blood/air partition coefficient[a]

[a]All partition coefficients used here represent ratios of concentrations expressed as mass per volume and are nominally dimensionless.

In all three models used here, the skin compartment is assumed to have the physiological properties of the stratum corneum only. This is a reasonable assumption for absorption of chloroform ($CHCl_3$), which is used as a test compound. $CHCl_3$ was chosen to take advantage of prior efforts of Gordon *et al.* (1998) and Corley *et al.* (1990, 2000). Gordon *et al.* (1998) performed experiments in which subjects were immersed in water containing $CHCl_3$ in hydrotherapy tubs while breathing purified air to eliminate inhalation exposure. Exhaled breath concentration of $CHCl_3$ was monitored during the roughly 0.5-h exposure period and postexposure. Water concentration (c. 90 ppb) and temperature (nominally 30°C, 35°C, and 40°C), and immersion time varied slightly across subjects. A total of 10 (five male, five female) volunteers participated, but not all subjects produced data at each of the target temperatures. Corley *et al.* (2000) analyzed these experiments after adapting their prior $CHCl_3$ PBPK model (Corley *et al.*, 1990) by adding a (CSTR) skin compartment.

The objective of this paper is to demonstrate potential differences in overall PBPK model performance when using the CSTR, approximate membrane (STL), and true membrane

Downloaded from https://academic.oup.com/toxsci/article-abstract/104/1/210/1721500
by Centers For Disease Control user
on 23 August 2018

TABLE 2
Temperature-Independent Model Parameter Values

Model parameter	Value	Source
Exposed skin surface area, A_{ex} (cm^2)	20,446	Corresponds to subject 7 in Gordon *et al.* (1998)
Body weight (kg)	79.4	Corresponds to subject 7 in Gordon *et al.* (1998)
Chemical concentration in air	0	Reported by Gordon *et al.* (1998)
Maximum metabolism rate, v_{max} (mg/kg/h)	93.2	Calculated from data reported in Lipscomb *et al.* (2003)
Water loss rate constant, k_{loss} (/h)	0	
Michaelis-Menten constant, K_m (mg/l)	0.016	Reported in Lipscomb *et al.* (2004)
Permeability coefficient, K_p (cm/h)	(Fitted)	Fitted by MCMC to observed breath data from Gordon *et al.* (1998) experiments
Volume of aqueous vehicle (l)	380	Reported by Gordon *et al.* (1998)
Partition coefficients		
Blood/air	7.4	Average of values reported by Steward *et al.* (1973) and Gargas *et al.* (1989)
Blood/water	2.04	Calculated from blood/air partition coefficient and Henry's law constant at 37°C per Staudinger & Roberts (2001)
Fat/blood	37.8	Calculated from data reported by Steward *et al.* (1973)
Liver/blood	2.3	Calculated from data reported by Steward *et al.* (1973)
Rapidly perfused tissue/blood	2.3	Calculated from data reported by Steward *et al.* (1973)
Slowly perfused tissue/blood	1.6	Calculated from data reported by Steward *et al.* (1973)
Stratum corneum/blood	14.1	Calculated using equations given in Roy *et al.* (1996)
Stratum corneum/water	28.7	Estimated using equation given in Bunge *et al.* (1995)
Body weight (%)		
Fat	23.1	Reported by Corley *et al.* (1990)
Liver	3.14	Reported by Corley *et al.* (1990)
Rapidly perfused tissue	3.27	Reported by Corley *et al.* (1990)
Slowly perfused tissue	61.4	Reported by Corley *et al.* (1990)
Stratum corneum	0.028	Assumes stratum corneum thickness of 10 μm

(FD) models of skin. If model predictions vary across the model types, values of any parameters, such as K_p that are estimated by fitting may also be model-dependent. Unless model-induced effects are either known to be negligible or understood and controlled, comparisons of apparent results across laboratories, species or techniques (e.g., *in vivo*/*in vitro*) may lead to incorrect conclusions regarding differences or lack thereof in values of parameters used to describe dermal phenomena.

MATERIALS AND METHODS

All three model versions, CSTR, STL, and FD, were created using Matlab 7.2 (The Mathworks, Natick, MA). All models were composed of differential equations representing the compartments shown schematically in Figure 1. The general approach used here is similar to that reported by Corley *et al.* (2000). Base equations describing the systemic distribution and elimination of a chemical are presented in Table 1. Those equations are consistent with the approach taken by Corley *et al.* as is the assumption that alveolar respiration accounts for 70 percent of total respiration (Ramsey and Andersen, 1984). Notable conceptual differences include (1) implementation of versions (discussed below) that do not model skin as a CSTR, (2) characterization of skin using properties of the stratum corneum rather than the whole skin, (3) inclusion of the kidney within richly perfused tissue rather than as a discreet compartment, and (4) restriction of $CHCl_3$ metabolism to the liver only. Corley *et al.* modeled the kidney discreetly to gain insight into potential toxicological effects that are not a topic of this paper. The contribution of the kidney to total metabolism was negligible and is therefore ignored here. In addition to these conceptual changes, numerical values of some input parameters and the manner in which cardiac output, ventilation rates, and blood flow to tissues were estimated for exposures at different temperatures differ from Corley *et al.* (2000). Corley *et al.* estimated metabolic parameters by extrapolation from rodent experiments. More recent human data reported by Lipscomb *et al.* (2003, 2004) are used here. Parameters for the models are shown in Tables 2 and 3. The skin/water partition coefficient was estimated using a formula relating the stratum corneum/water partition coefficient (K_{scw}) to K_{ow} (Bunge *et al.*, 1995):

$$\log K_{scw} = 0.74 \log K_{ow} \quad (1)$$

The skin/blood partition coefficient was calculated by dividing the skin/water partition coefficient by the blood/water partition coefficient. The blood/water partition coefficient was estimated as the product of the blood/air partition coefficient (average of values reported by Steward *et al.*, 1973 and Gargas *et al.*, 1989) and the Henry's law constant for $CHCl_3$ at body temperature. Cardiac output and blood flow to the skin were estimated using data from sources shown in Table 3. The density of all tissues was assumed to be 1 kg/l. Values of the permeability coefficient from water, K_p, were estimated individually for each model and bath water temperature by Markov chain Monte Carlo (MCMC) fitting to observed breath data from Gordon *et al.*'s trials using subject no. 7. Those calculations were conducted in WinBUGS 1.4.2 with BlackBox 1.5.

Movement of a chemical compound among water, skin, and blood compartments for the CSTR and STL model versions is depicted in Figure 2. The rate at which the chemical moves among the compartments is controlled by the rate constants (k_1, k_{-1}, k_2, and k_{-2}) and the concentration of the chemical in each compartment. Equations for the CSTR and STL model rate constants are shown in Table 4. The STL model mimics the membrane model for certain conditions (McCarley and Bunge, 1998, 2001). Equations for the exposed skin compartment for the CSTR and STL models are shown in Table 5. The

Downloaded from https://academic.oup.com/toxsci/article-abstract/104/1/210/1721500
by Centers For Disease Control user
on 23 August 2018

TABLE 3
Temperature-Dependent Model Parameter Values

Model parameter	Value		
Approximate exposure temperature (°C)	28[a]	35[a]	39[a]
Exposure time (h)	0.5[a]	0.497[a]	0.487[a]
$CHCl_3$ concentration (mg/l)	0.088[a]	0.0945[a]	0.0895[a]
Cardiac output (l/h)	384[b]	384[c]	522[c]
Alveolar respiration rate (l/h)	384[d]	384[e]	404[f]
Cardiac output (%)			
Fat	5.2[g]	5.2[g]	4.1[c,g]
Liver	22.7[g]	22.7[g]	18.0[c,g]
Rapidly perfused tissue	46.8[h]	46.3[i]	34.6[i,j]
Slowly perfused tissue	21.9[k]	21.9[k]	15.3[k]
Skin (stratum corneum)	3.5[c,l]	3.9[m]	28.1[c]

[a]Gordon *et al*. (1998) subject no. 7 trials.
[b]Equal to the 35°C baseline exposure scenario per Choukroun and Varene (1990).
[c]Reported by or estimated from Rowell (1974).
[d]Equal to the 35°C baseline exposure scenario per data reported in Cooper *et al*. (1976).
[e]Corley *et al*. (1990).
[f]Estimated from data reported in Cooper and Veale (1986).
[g]Estimated from data reported by Brown *et al*. (1997).
[h]Accounts for decrease in skin blood flow from 35°C baseline exposure scenario.
[i]Calculated from Corley *et al*. (1990) estimate of blood flow to nonrenal rapidly perfused tissue and Rowell (1974) estimate of blood flow to renal tissue.
[j]Calculated as the proportional decrease in total blood flow to rapidly perfused tissues from the decrease in blood flow to renal tissue reported by Rowell (1974).
[k]Accounts for remaining percent cardiac output after determining percent distributed to other tissues.
[l]Estimated from data reported by Roddie (1983).
[m]Charkoudian (2003).

membrane model utilizes a second-order FD scheme (Table 6). In the postexposure period, the external phase is air rather than water. Postexposure evaporation from the exposed skin is allowed by the models presented here. For a volatile compound such as $CHCl_3$, skin-side mass transfer resistance would be expected to control evaporation, and the exposure model equations will still apply if $C_w = 0$.

RESULTS

Concentration profiles of $CHCl_3$ in exhaled breath generated by the three models are displayed in Figure 3 as are breath data from Gordon *et al*. (subject no. 7, 39°C). In each case values of

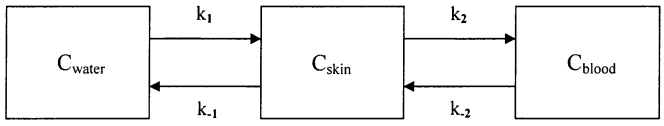

FIG. 2. Schematic diagram of the movement of a chemical compound among water, skin, and blood for a single skin compartment PBPK model (adapted from Reddy *et al*., 1998).

TABLE 4
Rate Constants for the CSTR and STL Models (Reddy *et al*., 1998)

	CSTR	STL
k_1	$K_p A_{ex}$	$\frac{3(2+\alpha_{sc})}{(3+\alpha_{sc})} K_p A_{ex}$
k_2	$\alpha_{sc} \frac{K_p A_{ex}}{P_{skw}}$	$\frac{2\alpha_{sc}}{(2+\alpha_{sc})} \frac{K_p A_{ex}}{P_{skw}}$
k_{-1}	$\frac{K_p A_{ex}}{P_{skw}}$	$\frac{4(3+3\alpha_{sc}+\alpha_{sc}^2)}{(2+\alpha_{sc})(3+\alpha_{sc})} \frac{K_p A_{ex}}{P_{skw}}$
k_{-2}	$\alpha_{sc} \frac{K_p A_{ex}}{P_{bw}}$	$\frac{3\alpha_{sc}}{(3+\alpha_{sc})} \frac{K_p A_{ex}}{P_{bw}}$

α_{sc} = ratio of blood clearance to absorption $= \frac{Q_{ba} \text{fcard}_{sk} P_{bw} C_f}{A_t K_p}$
K_p = permeability coefficient (cm/h)
A_{ex} = area of exposed skin (cm^2)
P_{skw} = skin/water partition coefficient
Q_{ba} = cardiac output (l/h)
fcard_{sk} = fraction of cardiac output going to skin
P_{bw} = blood/water partition coefficient
C_f = conversion factor (1000 cm^3/l)
A_t = total skin surface area (cm^2)

K_p were obtained by MCMC estimation using breath data from the approximately 30-min exposure period. The CSTR model predicts a peak $CHCl_3$ breath concentration of less than 7 ppb at the end of the exposure period. Both the STL and FD models predict higher peak breath concentrations. In the case of the FD model, the peak occurs shortly after the end of the 29-min exposure period (i.e., at about 31 min) due to continuing

TABLE 5
Equations for Exposed Skin Compartment in the CSTR and STL Models

CSTR model:

$$\frac{dC_{skex}}{dt} = \frac{Q_{bskex}}{V_{skex}} \left[C_{art} - \frac{C_{skex}}{P_{skb}} \right] + \left[\frac{K_p A_{ex}}{C_f V_{skex}} \right] \left[C_{water} - \frac{C_{skex}}{P_{skw}} \right]$$

STL model:

$$\frac{dC_{skex}}{dt} = \left[\frac{K_p \times A_{ex}}{C_f \times V_{skex}} \right] \times \left\{ \left[\frac{3 \times \alpha_{sc}}{(3+\alpha_{sc})} \times \frac{C_{bls}}{P_{bw}} - \frac{2 \times \alpha_{sc}}{(2+\alpha_{sc})} \times \frac{C_{skex}}{P_{skw}} \right] + \left[\frac{3 \times (2 \times \alpha_{sc})}{3+\alpha_{sc}} C_{water} - \frac{4 \times (3+3\alpha_{sc}+\alpha_{sc}^2)}{(2 \times \alpha_{sc}) \times (3+\alpha_{sc})} \times \frac{C_{skex}}{P_{skw}} \right] \right\}$$

C_{skex} = concentration of $CHCl_3$ in exposed skin (mg $CHCl_3$/l skin)
Q_{bskex} = blood flow to exposed skin (l/h)
V_{skex} = volume of exposed skin (l)
C_{art} = concentration of $CHCl_3$ in arterial blood (mg $CHCl_3$/l blood)
P_{skb} = skin/blood partition coefficient
K_p = permeability coefficient of $CHCl_3$ (cm/h)
A_{ex} = area of exposed skin (cm^2)
C_f = conversion factor (1000 cm^3/l)
C_{water} = concentration of $CHCl_3$ in water (mg $CHCl_3$/l water)
P_{skw} = skin/water partition coefficient
α_{sc} = ratio of blood clearance to absorption (see Table 4)
C_{bls} = concentration of $CHCl_3$ in blood leaving skin (mg $CHCl_3$/l blood)
P_{bw} = blood/water partition coefficient

Downloaded from https://academic.oup.com/toxsci/article-abstract/104/1/210/1721500
by Centers For Disease Control user
on 23 August 2018

TABLE 6
Finite-Difference Scheme for Membrane (FD) Model

At $j = 1$:
$$\frac{dC_{sk}(1)}{dt} = P_{skw}\frac{dC_{water}}{dt}$$

For $j = 2, n - 1$:
$$\frac{dC_{sk}(j)}{dt} = \frac{D}{\Delta x^2}\Big(C_{sk}(j-1) - 2C_{sk}(j) + C_{sk}(j+1)\Big)$$

At $j = n$:
$$\frac{dC_{sk}(n)}{dt} = \frac{D}{\Delta x^2}\Big(-C_{sk}(n-2) + 4C_{sk}(n-1) - 3C_{sk}(n)\Big) + \frac{Q_{bskex}}{A_{ex}\Delta x/2}\left(C_{art} - \frac{C_{sk}(n)}{P_{skb}}\right)$$

$C_{sk}(j)$ = concentration of $CHCl_3$ at skin node j
P_{skw} = skin/water partition coefficient
C_{water} = concentration of $CHCl_3$ in water (mg $CHCl_3$/l water)
n = number of skin nodes (number of layers + 1)
D = diffusivity in skin (cm^2/h)
Δx = thickness of a skin layer (cm)
Q_{bskex} = blood flow to exposed skin (l/h)
A_{ex} = area of exposed skin (cm^2)
C_{art} = concentration of $CHCl_3$ in arterial blood (mg $CHCl_3$/L blood)
P_{skb} = skin/blood partition coefficient

exhalation of previously absorbed $CHCl_3$. The CSTR model predicts immediate appearance of $CHCl_3$ in the exhaled breath upon initiation of exposure and immediate decline upon cessation. The STL and FD models predict more gradual appearance of $CHCl_3$ in the exhaled breath with the FD breath profile exhibiting a distinct initial lag period (i.e., delayed initial appearance of $CHCl_3$ in the breath). Both membrane models also predict more gradual decline of $CHCl_3$ in breath after exposure ends.

The membrane models also predict differing disposition of $CHCl_3$ (Figs. 4 and 5) than the CSTR model. In the CSTR output the cumulative mass of $CHCl_3$ transferred from the water into the skin is essentially the same as the mass transferred from the skin to blood, that is, storage of $CHCl_3$ in the skin is negligible (Fig. 4a). In contrast, the STL (Fig. 4b) and FD (Fig. 4c) models predict that skin-to-blood transfer lags water-to-skin transfer, leading to substantial accumulation of $CHCl_3$ in the skin at 30 min. The cumulative mass of $CHCl_3$ predicted to be transferred from water into skin by the membrane models is roughly double that predicted by the CSTR model during the exposure period, but the corresponding transfer from skin to blood in the first 30 min is roughly the same across the three models. Each of the models also predicts that roughly half of the $CHCl_3$ transferred from skin to blood would be accounted for by storage in compartments other than skin at the end of the exposure period. The remaining mass of $CHCl_3$ passing through the skin is approximately equally divided between metabolism and exhalation. Internal checks confirm that all three models conserve mass within a reasonable margin of error.

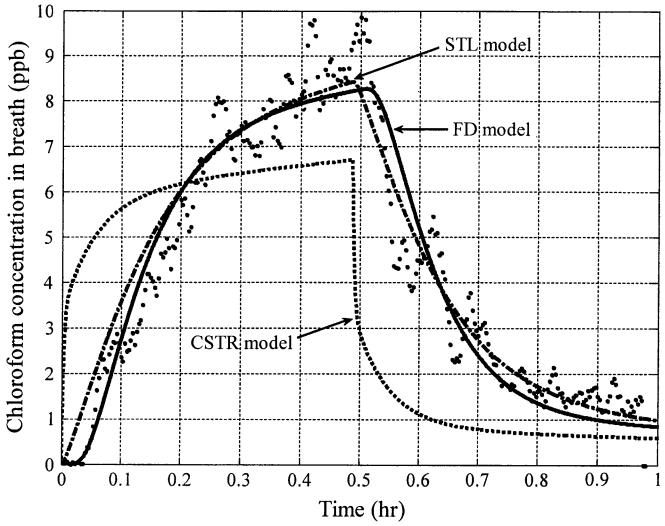

FIG. 3. Breath concentration profiles for the CSTR (dotted line), approximate membrane/STL (dot-dashed line), and membrane/FD (solid line) models using water permeability coefficients obtained by MCMC fit to 29-min exposure phase data from Gordon *et al.*'s (1998) subject no. 7 (39°C trial).

DISCUSSION

Because a CSTR model overestimates initial breath concentration, fitting of such a model to breath data will lead to underestimation of subsequent breath concentration. This effect is apparent in Figure 3. Some prior investigators have "manually" induced a lag in a CSTR skin model by starting simulations at $t > 0$. Although this tactic may produce an apparent improvement in fit initially, it has the effect of requiring that the actual exposure period be artificially shortened. Because the STL (approximate membrane) model is a modified CSTR, it also predicts instantaneous appearance of VOC in breath. However, the effect is dampened and more gradual. The true membrane (FD) model predicts a lag more consistent with the data shown in Figure 3. However, the FD model is computationally more expensive than the other two models. A potential advantage of the STL approach is that it requires only slightly more computing time than the CSTR model, but produces a result very similar to the FD model. In applications in which the model must be run repeatedly, such as MCMC fitting or other stochastic simulations, approximate membrane solutions may be very useful.

Overall absorbed doses predicted by the membrane models were larger than those predicted by the CSTR model. If chronic exposures are of primary interest, CSTR approaches may underestimate dose. Conversely if acute effects are of primary interest, CSTR approaches may overstate short-term dose. In effect, CSTR models dump penetrants into the blood stream very quickly. This phenomenon may be important in scenarios in which the doses being evaluated are near those that produce acute effects.

Permeability coefficients estimated using the various models are presented in Table 7. The three approaches used here are contrasted for each of the Gordon *et al.* exposure temperatures. Dependence of the estimated K_p on both model type and

Downloaded from https://academic.oup.com/toxsci/article-abstract/104/1/210/1721500
by Centers For Disease Control user
on 23 August 2018

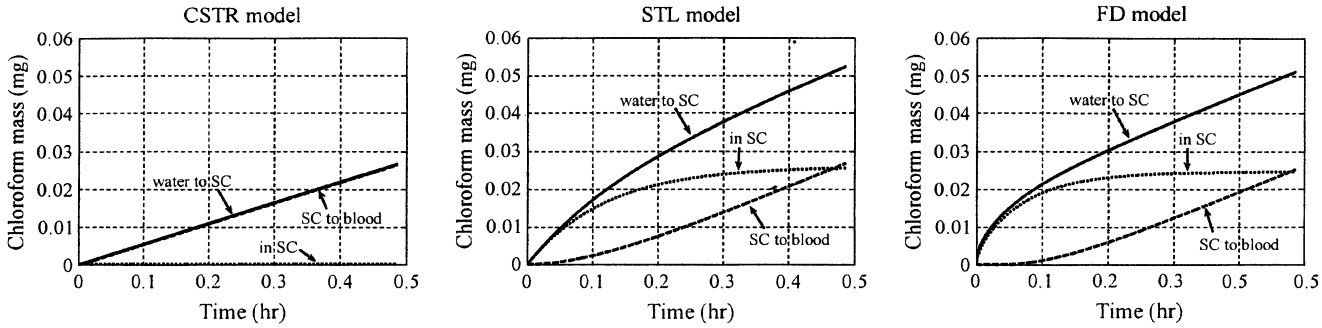

FIG. 4. (a, b, and c) Mass balance on skin for the CSTR, approximate membrane (STL), and membrane (FD) models during the 29-min exposure to 39°C water. The solid, dotted, and dashed lines represent the net mass (mg) of $CHCl_3$ transferred from water to exposed stratum corneum, mass (mg) of $CHCl_3$ stored in the stratum corneum, and mass (mg) of $CHCl_3$ transferred from stratum corneum to blood, respectively.

temperature is evident. For the 39°C case, estimates derived from membrane approaches were about 25% larger than the value produced for the CSTR model. For the lower temperatures, K_p estimates from the membrane approaches were 1.5–5 times the CSTR estimates. The 28°C values are of particular interest because the data on which the Potts-Guy model is based were obtained *in vitro* at or near 30°C. In this case, values of K_p obtained from fitting the STL and FD models at the lowest experimental temperature are both closer to the Potts-Guy estimate than the value obtained from fitting the CSTR model. This is a logical outcome because the Potts-Guy estimates are based on membrane interpretation of *in vitro* data. Failure to match a K_p derived from (similar temperature) human *in vivo* data to the Potts-Guy estimate should therefore not be assumed to be evidence of *in vivo/in vitro* differences as it could also be explained by dissimilarity of modeling approaches.

Substantially elevated K_p estimates at the higher temperatures are reported here, a finding consistent with the prior interpretation of Corley *et al.* (2000). This result is attributable to higher observed breath concentrations at higher water temperatures and is relatively insensitive to assumptions regarding blood flow rates. Increasing total cardiac output and relative blood flow to the skin with increasing temperature, as assumed here, have countervailing effects on the magnitude of K_p required to match the breath data in all three models. A finding of substantially elevated K_p suggests that the ratio of dermal to ingestion exposure to $CHCl_3$ (and by extension to other VOCs in water) may be much greater than estimated in EPA guidance (U.S. EPA, 2004), in which dermal exposure calculated using the modified Potts-Guy regression is contrasted with exposure associated with consumption of 2 l of drinking water.

In summary, the predictions of PBPK models that incorporate a skin compartment are generally sensitive to the form of the skin model used and the temperature of the external medium. If values of the permeability coefficient, K_p, are backfit from experimental data, these effects should be considered.

FUNDING

U.S. Environmental Protection Agency (cooperative agreement R-82963201); and Centers for Disease Control and

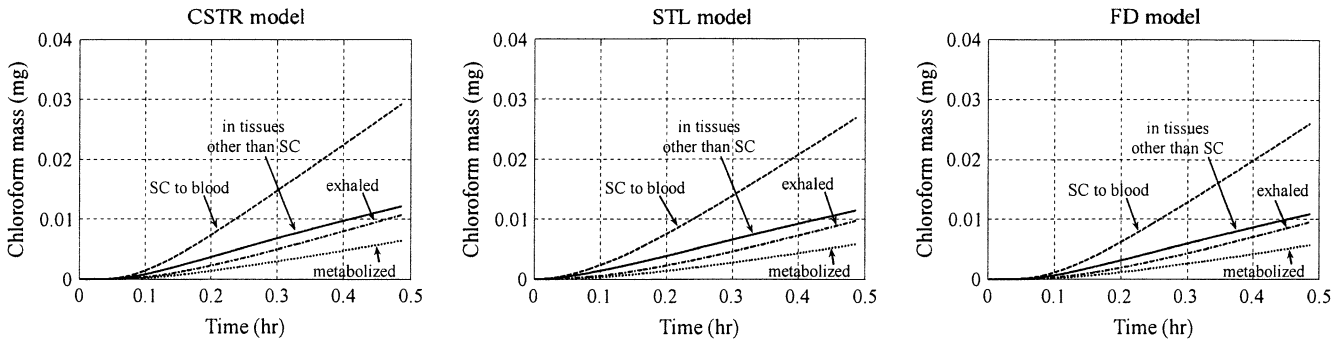

FIG. 5. (a, b, and c) Disposition of absorbed mass as predicted by the CSTR, approximate membrane (STL), and membrane (FD) models during the 29-min exposure to 39°C water. The dashed, solid, dot-dashed, and dotted lines represent the net mass (mg) of $CHCl_3$ transferred from exposed stratum corneum to the bloodstream, mass (mg) of $CHCl_3$ stored in compartments other than exposed stratum corneum, mass (mg) of $CHCl_3$ exhaled, and mass (mg) of $CHCl_3$ metabolized, respectively.

Downloaded from https://academic.oup.com/toxsci/article-abstract/104/1/210/1721500
by Centers For Disease Control user
on 23 August 2018

TABLE 7
Estimates of K_p (cm/h)

Source of estimate	Model	Approximate water temperature (°C) 28	35	39
This paper[a]	CSTR	0.0018	0.022	0.042
	STL	0.0034	0.033	0.053
	FD	0.0089	0.031	0.052
Modified Potts-Guy regression (U.S. EPA, 2004)		0.0068		

[a]By fitting breath data from Gordon *et al.*'s (1998) subject no. 7. Temperatures reflect experimental conditions.

Prevention/National Institute for Occupational Safety and Health (training grant T42/CCT010418-11) to A.M.N. and J.A.S. and (T42/OH008433) to K.L.S.

ACKNOWLEDGMENTS

Material presented here has not been reviewed by EPA and no Agency endorsement should be inferred. We thank S. Gordon for sharing data.

REFERENCES

Brown, R. P., Delp, M. D., Lindstedt, S. L., Rhomberg, L. R., and Beliles, R. P. (1997). Physiological parameter values for physiologically based pharmacokinetic models. *Toxicol. Ind. Health* **13,** 407–484.

Bunge, A. L., Cleek, R. L., and Vecchia, B. E. (1995). A new method for estimating dermal absorption from chemical exposure. 3. Compared with steady-state methods for prediction and data analysis. *Pharm. Res.* **12,** 972–982.

Charkoudian, N. (2003). Skin blood flow in adult human thermoregulation: how it works, when it does not, and why. *Mayo Clin. Proc.* **78,** 603–612.

Choukroun, M., and Varene, P. (1990). Adjustments in oxygen transport during head-out immersion in water at different temperatures. *Respir. Physiol.* **75,** 255–265.

Cooper, K. E., Martin, S., and Riben, P. (1976). Respiratory and other responses in subjects immersed in cold water. *J. Appl. Physiol.* **40,** 903–910.

Cooper, K. E., and Veale, W. L. (1986). Effects of temperature on breathing. In *Handbook of Physiology, Section 3: The Respiratory System,* (N. S. Cherniack and J. G. Widdicombe, Eds.), Vol. 2, pp. 691–702, American Physiological Society, Bethesda, MD.

Corley, R. A., Gordon, S. M., and Wallace, L. A. (2000). Physiologically based pharmacokinetic modeling of the temperature-dependent dermal absorption of chloroform by humans following bath water exposures. *Toxicol. Sci.* **53,** 13–23.

Corley, R. A., Mendrala, A. L., Smith, F. A., Staats, D. A., Gargas, M. L., Conolly, R. B., Andersen, M. E., and Reitz, R. H. (1990). Development of a Physiologically based pharmacokinetic model for chloroform. *Toxicol. Appl. Pharmacol.* **103,** 512–517.

Gargas, M. L., Burgess, R. J., Voisard, D. E., Cason, G. H., and Andersen, M. E. (1989). Partition coefficients of low-molecular-weight volatile chemicals in various liquids and tissues. *Toxicol. Appl. Pharmacol.* **98,** 87–99.

Gordon, S. M., Wallace, L. A., Callahan, P. J., Kenny, D. V., and Brinkman, M. C. (1998). Effect of water temperature on dermal exposure to chloroform. *Environ. Health Perspect.* **106,** 337–345.

Lipscomb, J. C., Barton, H. A., Tornero-Velez, R., Evans, M. V., Alcasey, S., Snawder, J. E., and Laskey, J. (2004). The metabolic rate constants and specific activity of human and rat hepatic cytochrome P-450 2E1 toward toluene and chloroform. *J. Toxicol. Environ. Health A* **67,** 537–553.

Lipscomb, J. C., Teuschler, L. K., Swartout, J. C., Striley, C. A. F., and Snawder, J. E. (2003). Variance of microsomal protein and cytochrome P450 2E1 and 3A forms in adult human liver. *Toxicol. Mech. Methods* **13,** 45–51.

McCarley, K. D., and Bunge, A. L. (1998). Physiologically relevant one-compartment pharmacokinetic models for skin. 1. Development of models. *J. Pharm. Sci.* **87,** 470–481.

McCarley, K. D., and Bunge, A. L. (2001). Pharmacokinetic models of dermal absorption. *J. Pharm. Sci.* **90,** 1699–1719.

Poet, T. S., Corley, R. A., Thrall, K. D., Edwards, J. A., Tanojo, H., Weitz, K. K., Hui, X., Maibach, H. I., and Wester, R. C. (2000a). Assessment of the percutaneous absorption of trichloroethylene in rates and humans using MS/MS real-time breath analysis and physiologically based pharmacokinetic modeling. *Toxicol. Sci.* **56,** 61–72.

Poet, T. S., Thrall, K. D., Corley, R. A., Hui, X., Edwards, J. A., Weitz, K. K., Maibach, H. I., and Wester, R. C. (2000b). Utility of real time breath analysis and physiologically based pharmacokinetic modeling to determine the percutaneous absorption of methyl chloroform in rats and humans. *Toxicol. Sci.* **54,** 42–51.

Ramsey, J. C., and Andersen, M. E. (1984). A physiologically based description of the inhalation pharmacokinetics of styrene in rats and humans. *Toxicol. Appl. Pharmacol.* **73,** 59–75.

Reddy, M. B., McCarley, K. D., and Bunge, A. L. (1998). Physiologically relevant one-compartment pharmacokinetic models for skin. 2. Comparison of models when combined with a systemic pharmacokinetic model. *J. Pharm. Sci.* **87,** 482–490.

Roddie, I. C. (1983). Circulation to skin and adipose tissue. In *Handbook of Physiology, Section 2: The Cardiovascular System,* (J. T. Shepherd and F. M. Abboud, Eds.), Vol. 3, pp. 285–317. American Physiological Society, Bethesda, MD.

Rowell, L. B. (1974). Human cardiovascular adjustments to exercise and thermal stress. *Physiol. Rev.* **54**(1), 75–159.

Roy, A., Weisel, C. P., Lioy, P. J., and Georgopoulos, P. G. (1996). A distributed parameter physiologically-based pharmacokinetic model for dermal and inhalation exposure to volatile organic compounds. *Risk Anal.* **16,** 147–160.

Scheuplein, R. J. (1972). Properties of the skin as a membrane. *Adv. Biol. Skin* **12,** 125–152.

Staudinger, J., and Roberts, P. V. (2001). A critical compilation of Henry's law constant temperature dependence relations for organic compounds in dilute aqueous solutions. *Chemosphere* **44,** 561–576.

Steward, A., Allott, P. R., Cowles, A. L., and Mapleson, W. W. (1973). Solubility coefficients for inhaled anaesthetics for water, oil and biological media. *Br. J. Anaesth.* **45,** 282–293.

Thrall, K. D., Weitz, K. K., and Woodstock, A. D. (2002). Use of real-time breath analysis and physiologically based pharmacokinetic modeling to

Downloaded from https://academic.oup.com/toxsci/article-abstract/104/1/210/1721500
by Centers For Disease Control user
on 23 August 2018

evaluate dermal absorption of aqueous toluene in human volunteers. *Toxicol. Sci.* **68,** 280–287.

Thrall, K., and Woodstock, A. (2003). Evaluation of the dermal bioavailability of aqueous xylene in F344 rats and human volunteers. *J. Toxicol. Environ. Health A* **66,** 1267–1281.

U. S. EPA. (2004). Risk assessment guidance for superfund (RAGS). *Human health evaluation manual, part E, supplemental guidance for dermal risk assessment.* Vol. 1, EPA/540/R/99/005.

Xu, X., and Weisel, C. P. (2005). Dermal uptake of chloroform and haloketones during bathing. *J. Expo. Anal. Environ. Epidemiol.* **15,** 289–296.

Downloaded from https://academic.oup.com/toxsci/article-abstract/104/1/210/1721500
by Centers For Disease Control user
on 23 August 2018